No. 349 JULY 2015

T.W.I.T.T. NEWSLETTER

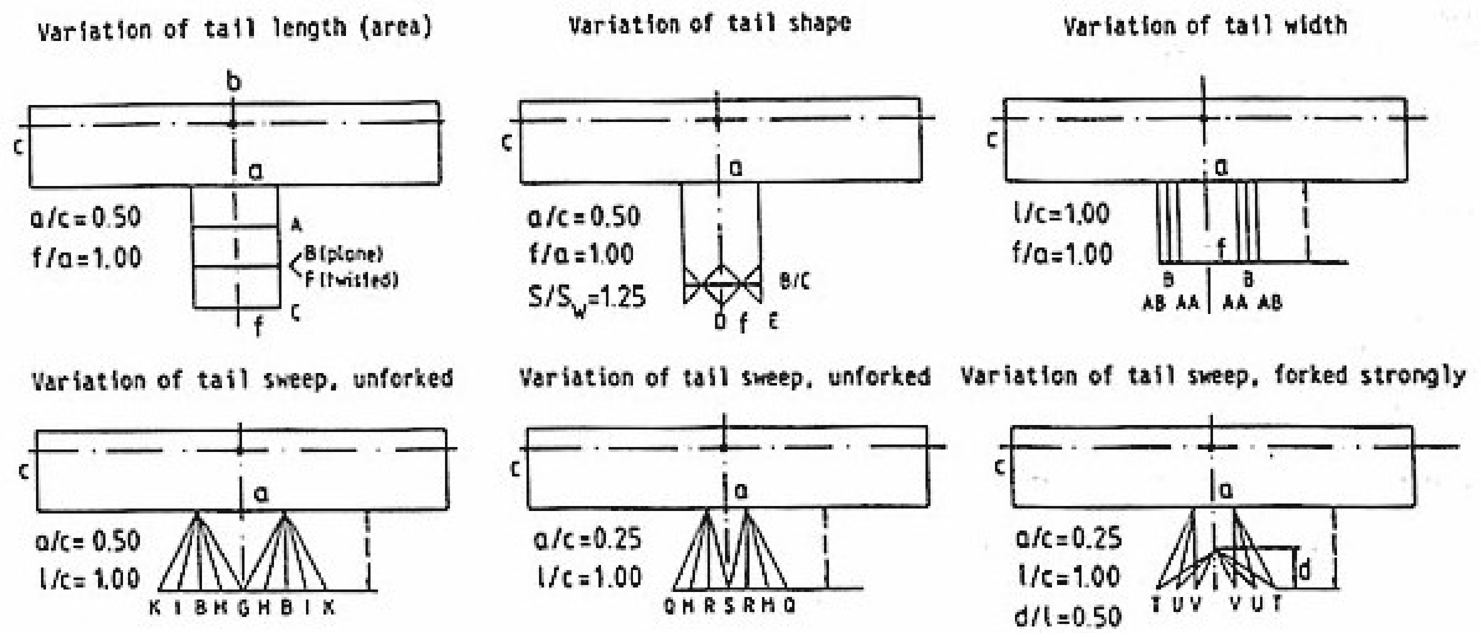
Variation of tail length (area)

Variation of tail shape

Variation of tail width

Variation of tail sweep, unforked

Variation of tail sweep, unforked

Variation of tail sweep, forked strongly

Illustration example from a technical paper on the tail effects in birds that is started in this issue on page 2.

T.W.I.T.T.
The Wing Is The Thing
P.O. Box 20430
El Cajon, CA 92021

The number after your name indicates the ending year and month of your current subscription, i.e., **1507** means this is your last issue unless renewed.

TWITT
THE WING IS THE THING

THE WING IS THE THING (T.W.I.T.T.)

T.W.I.T.T. is a non-profit organization whose membership seeks to promote the research and development of flying wings and other tailless aircraft by providing a forum for the exchange of ideas and experiences on an international basis.

T.W.I.T.T. Officers:

President: Andy Kecskes (619) 980-9831
Treasurer:
Editor: Andy Kecskes
Archivist: Gavin Slater

The **T.W.I.T.T.** office is located at:
Hanger A-4, Gillespie Field, El Cajon, California.
Mailing address: P.O. Box 20430
El Cajon, CA 92021

(619) 589-1898 (Evenings – Pacific Time)
E-Mail: twitt@pobox.com
Internet: http://www.twitt.org
Members only section: ID – **20issues10**
Password – **twittmbr**

Subscription Rates: $20 per year (US)
$30 per year (Foreign)
$23 per year US electronic
$33 per year foreign electronic

Information Packages: $3.00 ($4 foreign)
(includes one newsletter)

Single Issues of Newsletter: $1.50 each (US) PP
Multiple Back Issues of the newsletter:
$1.00 ea + bulk postage

Foreign mailings: $0.75 each plus postage

Wt/#Issues	FRG	AUSTRALIA	AFRICA
1oz/1	1.75	1.75	1.00
12oz/12	11.00	12.00	8.00
24oz/24	20.00	22.00	15.00
36oz/36	30.00	32.00	22.00
48oz/48	40.00	42.00	30.00
60oz/60	50.00	53.00	37.00

Meetings are held on the third Saturday of every other month (beginning with January), at 1:30 PM, at Hanger A-4, Gillespie Field, El Cajon, California (first row of hangers on the south end of Joe Crosson Drive (#1720), east side of Gillespie or Skid Row for those flying in).

TABLE OF CONTENTS

PRESIDENT'S CORNER

It was nice last month having a "real" article for the newsletter, but there weren't any on hand for this issue. So I am continuing to digitize some of the technical articles that we have in the archives. These are generally photo copies of the originals or other copies so they are not perfectly clear. I have made whatever adjusts I could with my available software to make them as readable as possible. If you have trouble with the printed version you can always go to the members only section of the website and open up the PDF version. You can then push it out to about 125% to make it easier to read. The user ID and password on in the column to the left so it is easy to gain access to the electronic version.

This month I will start with the first half of a paper on "Aerodynamic Investigations on Tailless Effects in Birds" by D. Hummel originally published in 1992. This was donated to TWITT by our long time member Karl Sanders, who was a constant contributor until his passing some years ago.

This is a ten-page paper so the last part will fit easily into the August issue. However, don't let this deter you from sending in any questions or stories you would like to share since I am sure I can make room for them.

Andy

Z. Flugwiss. Weltraumforsch. 16 (1992) 159–168 © Springer-Verlag 1992

ZFW Zeitschrift für Flugwissenschaften und Weltraumforschung

Aerodynamic investigations on tail effects in birds

D. Hummel, Braunschweig

Summary: For a wing with control devices in the form of inboard aft extensions of the planform, representing the tail of a bird, the aerodynamic characteristics have been analyzed. In the 1.3 m low-speed windtunnel of the Institut für Strömungsmechanik at TU Braunschweig an experimental program has been carried out on an $A = 5$ rectangular wing for a large variety of control surfaces attached to the trailing-edge. Length, width, area, lateral spreading as well as fork deepness of the tail have been altered systematically. In addition deflections ε of the control surfaces up and down have been investigated, and for one planform shape also a twisted tail has been considered. Three- and six-component measurements have been carried out and the contributions of the various devices to stability and control have been determined.

By adding small control surfaces to the wing longitudinal stability is improved. With increasing length, corresponding to increasing area, of the tail the longitudinal stability ($-\mathrm{d}c_m/\mathrm{d}c_L$) rises considerably whereas the control effectivenesses $\mathrm{d}c_L/\mathrm{d}\varepsilon$ and $\mathrm{d}c_m/\mathrm{d}\varepsilon$ remain constant. Lateral spreading of the tail without and with simultaneous increase of the control surface area leads to increased stability and control effectiveness. In forked tails the relative increase of stability and control effectiveness is larger than for unforked tails. In symmetrical flow the tail of a bird acts as a horizontal stabilizer and as an elevator in the same way as in conventional airplanes.

Six-component measurements show for a twisted tail an increase of lateral stability which is independent of the sense of rotation of the tail. On the other hand twisting of a loaded tail leads to a side force, a rolling and a yawing moment which depend on the sense of rotation in combination with the sign of the loading and which contribute to lateral control. In birds lateral stability and control is achieved in an unconventional manner by a twisted tail, which replaces the vertical fin and the rudder of conventional airplanes.

Aerodynamische Untersuchungen über die Wirkungsweise des Schwanzes bei Vögeln

Übersicht: Es wurden die aerodynamischen Eigenschaften eines Flügels mit Steuerflächen untersucht, die eine rückwärtige Verlängerung des Flügelgrundrisses im Innenbereich darstellen und die dem Schwanz von Vögeln entsprechen. Im 1,3 m Niedergeschwindigkeits-Windkanal des Instituts für Strömungsmechanik der TU Braunschweig wurde ein Experimentalprogramm an einem Rechteckflügel mit dem Seitenverhältnis $A = 5$ durchgeführt, an dessen Hinterkante eine große Zahl verschiedener Steuerflächen angeordnet waren. Dabei wurden Länge, Breite, Fläche und Spreizung sowie die Tiefe einer Gabelung des Schwanzes systematisch variiert. Außerdem wurden Ausschläge der Steuerflächen nach oben und unten untersucht, und für eine Grundrißform wurde auch der Einfluß einer Verwindung des Schwanzes betrachtet. Es wurden Drei- und Sechskomponentenmessungen durchgeführt, und daraus wurden die Beiträge der verschiedenen Steuerflächenanordnungen zur Stabilität und zu den Steuerwirksamkeiten bestimmt.

Schon durch kleine Steuerflächen wird die Längsstabilität der Konfiguration verbessert. Mit wachsender Länge und damit auch der Fläche des Schwanzes nimmt die Längsstabilität ($-\mathrm{d}c_m/\mathrm{d}c_L$) stark zu, während die Steuerwirksamkeiten $\mathrm{d}c_L/\mathrm{d}\varepsilon$ und $\mathrm{d}c_m/\mathrm{d}\varepsilon$ praktisch unverändert bleiben. Eine Spreizung des Schwanzes ohne und mit gleichzeitiger Vergrößerung der Steuerfläche führt zu einer Zunahme der Stabilität und der Steuerwirksamkeiten. Bei gegabelten Steuerflächen ist dieser Zuwachs bei Spreizung größer als bei ungegabelten Steuerflächen. Bei symmetrischer Strömung wirkt der Schwanz der Vögel in gleicher Weise wie das Höhenleitwerk und das Höhenruder bei konventionellen Flugzeugen.

Die Sechskomponentenmessungen zeigen für verdrehte Steuerflächen, daß dadurch eine Vergrößerung der Richtungsstabilität erreicht wird, die von der Richtung der Verdrehung unabhängig ist. Andererseits führt das Verdrehen einer aerodynamisch belasteten Steuerfläche je nach Belastungsrichtung und Drehsinn des Ausschlages zu einer Seitenkraft, zu einem Roll- und einem Giermoment, wodurch eine Seitensteuerung zustande kommt. Bei Vögeln werden Richtungsstabilität und Seitensteuerung in unkonventioneller Weise durch einen verdrehten Schwanz bewirkt, der das Seitenleitwerk und das Seitenruder eines konventionellen Flugzeuges ersetzt.

List of Symbols

$\Lambda_W = A = b/c$	Aspect ratio of the wing without tail
N_{25W}	Geometric neutral point of the wing located on the centre line at $c/4$
$Re = V \cdot c/\nu$	Reynolds number
$S_W = b \cdot c$	Wing area
S_T	Tail area
$S = S_W + S_T$	Total area
V	Free stream velocity
A to Z, AA, AB	Notations for the different tail shapes according to Fig. 4
a	Half width of the tail at its base
b	Wing span
c	Wing chord
$c^*(y)$	Local chord of the wing-tail-configuration, consisting of the wing chord c in each section $y =$ const. plus contributions from the tail in inner sections $y =$ const.
$\bar{c} = \frac{1}{S}\int_{-s}^{+s} c^{*2}(y)\,\mathrm{d}y$	Mean aerodynamic chord
$c_D = 2D/\varrho V^2 S$	Drag coefficient[1]

Prof. Dr.-Ing. D. Hummel, Institut für Strömungsmechanik, Technische Universität Braunschweig, Bienroder Weg 3, W-3300 Braunschweig/FRG

[1] Data reduction with respect to the experimental coordinate system according to Fig. 5. Reference point for the moments is the geometric neutral point of the wing N_{25W}, signs of the moments according to Fig. 5.

$c_L = 2L/\varrho V^2 S$	Lift coefficient[2]
$c_Y = 2Y/\varrho V^2 S$	Sideforce coefficient[2]
$c_{L\varepsilon} = dc_L/d\varepsilon$	Tail effectiveness related to changes in lift due to deflections ε
$c_l = 4R/\varrho V^2 S b$	Rolling moment coefficient[1]
$c_m = 2M/\varrho V^2 S \bar{c}$	Pitching moment coefficient[1]
$c_{m\varepsilon} = dc_m/d\varepsilon$	Tail effectiveness related to changes in pitching moment due to deflections ε
$c_n = 4N/\varrho V^2 S b$	Yawing moment coefficient[1]
d	Fork deepness
f	Half width of the tail at its tip
l	Length of the tail
$s = b/2$	Wing half-span
x, y, z	Wing-fixed coordinate system according to Fig. 3
α	Angle of attack (Fig. 5)
β	Angle of sideslip (Fig. 5)
δ	Angle of twist at the tailing-edge of the tail, rotation around the centre line of the tail (Fig. 3)
ε	Deflection angle of the tail (Fig. 3)
ε_0	Basic deflection angle of the tail at $\varepsilon = 0°$. Angle between the airfoil's mean line at the trailing-edge of the wing and the plane $z = 0$
ϑ	Spreading angle of the tail (Fig. 3)
ϱ	Density of the air
ν	Kinematic viscosity of the air

1 Introduction

Stability and control of conventional airplanes are maintained by small additional lifting surfaces which are usually positioned downstream of the wing. A horizontal wing stabilizes the longitudinal motion and a flap at this wing acts as an elevator to control the pitching moment. Concerning the lateral motion a vertical fin leads to increased directional stability and a rudder at this fin is used to control the yawing moment, whereas control of the rolling moment is mainly achieved by deflections of the ailerons.

Recently the demand for vanishing radar signal has led to new aircraft shapes which have so-called "stealth" or "low observable (LO)" characteristics. Apart from special designs for the inlet and the exhaust systems of the engines and absolutely sharp leading-edges of the wing, the basic challenge in the design of this kind of aircraft is the reduction or the absence of a vertical fin. Aircraft shapes of this kind are the all-wing stealth bomber Northrop B-2, shown in Fig. 1, taken from [1], as well as the stealth fighter Lockheed F-117. Some designs for the Advanced Tactical Fighter (ATF) competition such as the Lockheed YF-22 and the Northrop YF-23 show also reduced fins with respect to their stealth capabilities. The flying wing according to Fig. 1 exhibits an inboard aft extension of the basic swept wing planform. This extension is relatively wide in spanwise direction and according to [1] it shows a saw-toothed trailing-edge related to the demand for additional control surfaces for flutter damping.

Very similar shapes occur in nature. Almost all birds are equipped with a tail according to Fig. 2. This tail is normally attached to the trailing-edge of the wing and it may be regarded as an inboard aft extension of the basic wing. Furthermore, at a first glance no bird has a vertical fin for directional stabilization and control. Therefore some basic aerodynamics of modern stealth aircraft and of birds are virtually the same and the question arises how stability and control are maintained in these configurations.

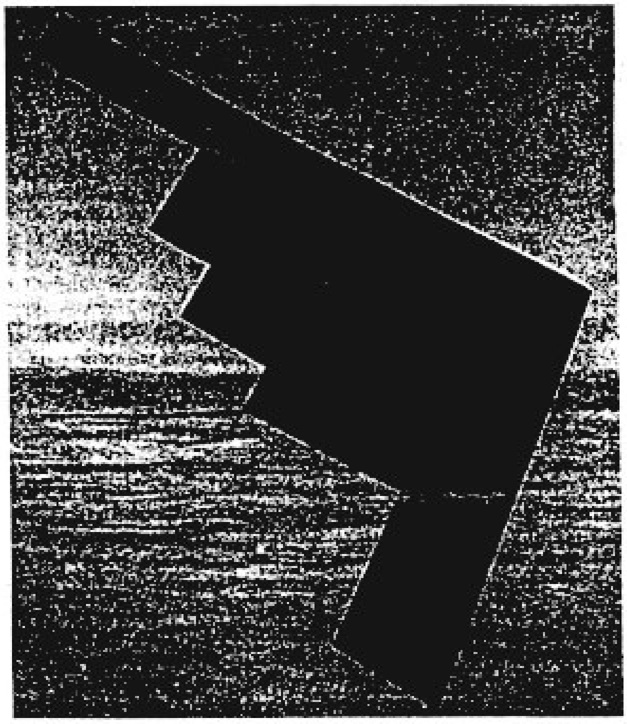

Fig. 1. All-wing stealth aircraft Northrop B-2 without vertical fin [1]

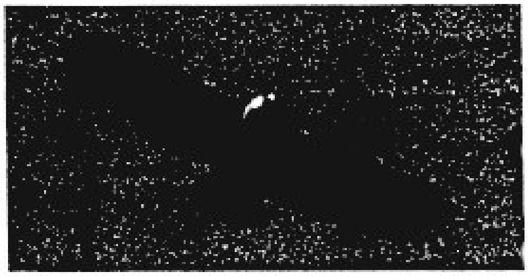

Fig. 2. Soaring Lesser-Spotted Eagle (Aquila pomarina)

In the aeronautical science there exist no systematic investigations on the aerodynamics of inboard aft extensions of a wing, see e.g. [2]. In the biological science it is common understanding since a long time [3–8] that deflections of the tail up and down act as an elevator to control the longitudinal motion. The effects of length, size and shape of the tail relative to the wing on the control effectiveness are unknown and detailed investigations on this subject are missing. Concerning lateral control twisting of the tail has been explained as a device to produce a rolling moment [5, 7, 8] and other effects have not yet been discussed so far. The important contribution of a tail to longitudinal and directional stability has not been considered. Therefore the present knowledge on the aerodynamic effects of a bird's tail is at low standard and systematic investigations on this subject are needed.

2 Experimental set-up and test program

2.1 *Windtunnel model*

The measurements have been carried out on a rectangular wing of aspect ratio $A_W = b/c = 5$ with a NACA 3412 airfoil

---

[2] Data reduction with respect to the experimental coordinate system according to Fig. 5. Reference point for the moments is the geometric neutral point of the wing N_{25W}, signs of the moments according to Fig. 5.

according to Fig. 3. This wing was equipped with a series of 26 different tails, in which the following dimensionless tail-parameters have been varied systematically:

1) Size (area ratio)	$\frac{S}{S_W} = \frac{S_W + S_T}{S_W}$
2) Length	l/c
3) Base width	a/c or a/b
4) Tip width or sweep	f/a or ϑ
5) Fork deepness	d/l

For any tail which is bordered by straight lines according to Fig. 3 the shape is prescribed independently by four of these parameters (e.g. 2, 3, 4, 5) whereas the remaining fifth parameter (e.g. 1) is a dependent one.

The tail shapes investigated in the present experimental program are shown in Fig. 4. The geometric data of these wing-tail-combinations may be taken from Table 1. In Fig. 4 the tails are ordered in subseries in order to show the constant and the varied parameters:

Series A/B/C: Variation of tail length (and area) for unswept tails of constant width.

Series (B + C)/D/E: Variation of tail shape (trailing-edge form) for unswept tails of constant width. A forked and a wedge-shaped tail are compared with a square cut one which is interpolated between *B* and *C*, all having the same area.

Series R/AA/B/AB: Variation of tail width (and area) for unswept tails of constant length.

Series G/H/B/I/K: Variation of tail sweep (and area) for constant length and (large) base width. This series is a rather realistic one related to shapes and functions in birds.

Series L/M/N/B/O/P: Variation of tail sweep (and area) for constant length and (large) tip width.

Series R/H/Z: Variation of tail sweep (and area) for constant length and (narrow) tip width.

Series S/R/M/Q: Variation of tail sweep (and area) for constant length and (narrow) base width of unforked tails. This series is the most realistic one related to shapes and function in birds; see Fig. 2.

Series Y/X/W: Variation of tail sweep (and area) for constant length and (narrow) base width for weakly forked tails.

Series V/U/T: Variation of tail sweep (and area) for constant length and (narrow) base width for strongly forked tails.

A comparison of the last three series describes the effect of forking the tail. Due to the very detailed variation of the dimensionless parameters according to Table 1 also series of tails with constant area and variation of sweep and base width can be set up. All the tails of this series were plane. They were manufactured from thin sheet metal and attached to the wing trailing-edge in such a way that the plane of the tail was directed tangential to the mean line of the airfoil

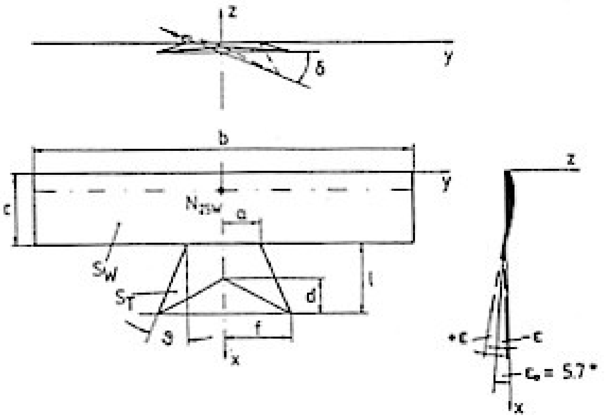

Fig. 3. Wing-tail-configuration. Notations and parameters

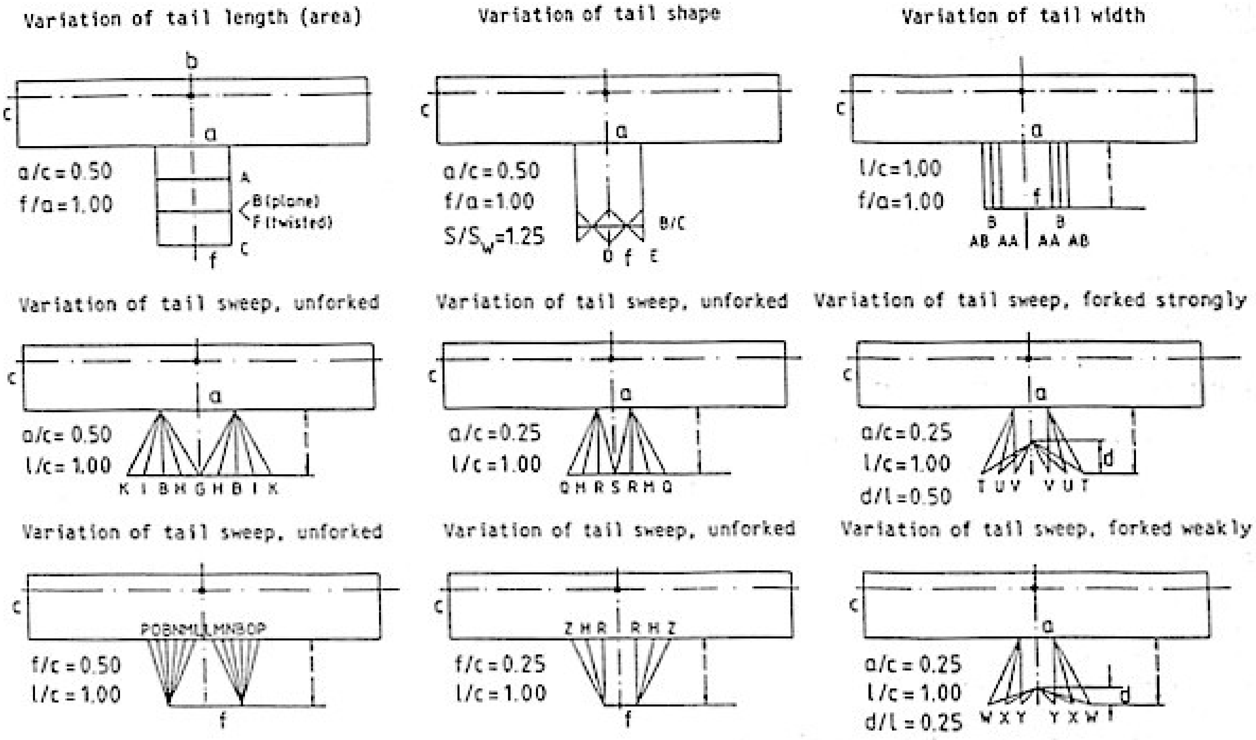

Fig. 4. Series of tail shapes on a rectangular wing, *A* = 5, airfoil NACA 3412. (Notations *A* to *Z*, *AA* and *AB*)

Table 1. Geometric data of the wing-tail-configurations

Tail shape	Mean aerod. chord, $\bar{c}/c$	Area S/S_W	Length l/c	Base width a/c	Tip width f/a	Sweep ϑ [°]	Fork deepness, d/l
A	1.1364	1.1000	0.50	0.500	1.00	0	0
B ≡ *F*	1.3333	1.2000	1.00	0.500	1.00	0	0
C	1.5769	1.3000	1.50	0.500	1.00	0	0
D	1.4533	1.2500	(1.25)	0.500	1.00	0	0
E	1.4533	1.2500	(1.25)	0.500	1.00	0	0
G	1.1515	1.1000	1.00	0.500	0	− 26.6	0
H	1.2464	1.1500	1.00	0.500	0.50	− 14.0	0
I	1.3867	1.2500	1.00	0.500	1.50	14.0	0
K	1.4359	1.3000	1.00	0.500	2.00	26.6	0
L	1.2000	1.1250	1.00	0.125	4.00	20.5	0
M	1.2464	1.1500	1.00	0.250	2.00	14.0	0
N	1.2908	1.1750	1.00	0.375	1.33	7.1	0
O	1.3605	1.2250	1.00	0.625	0.80	− 7.1	0
P	1.3867	1.2500	1.00	0.750	0.67	− 14.0	0
Q	1.3056	1.2000	1.00	0.250	3.00	26.6	0
R	1.1818	1.1000	1.00	0.250	1.00	0	0
S	1.0794	1.0500	1.00	0.250	0	− 14.0	0
T	1.1679	1.1250	1.00	0.250	3.00	26.6	0.50
U	1.1439	1.1000	1.00	0.250	2.00	14.0	0.50
V	1.1240	1.0750	1.00	0.250	1.00	0	0.50
W	1.2336	1.1625	1.00	0.250	3.00	26.6	0.25
X	1.1926	1.1250	1.00	0.250	2.00	14.0	0.25
Y	1.1513	1.0875	1.00	0.250	1.00	0	0.25
Z	1.3056	1.2000	1.00	0.750	0.33	− 26.6	0
AA	1.2609	1.1500	1.00	0.375	1.00	0	0
AB	1.4000	1.2500	1.00	0.625	1.00	0	0

NACA 3412 which is inclined against the plane $z = 0$ there at an angle of $\varepsilon_0 = 5.7°$ according to Fig. 3. This basic position of the tail is considered to be the normal position without deflection, $\varepsilon = 0°$. In order to get the effectiveness of these tails as elevators all these tails were measured also for deflections up and down, $\varepsilon = \pm 5°$. For this purpose the plane thin sheet metal tails were bended up and down around the wing's trailing-edge.

The basic planform of this series of tails is form *B*. Tails of this shape have also been tested as twisted tails *F*. For this purpose the straight trailing-edge of the tail was rotated about the centre line of the plane tail at an angle δ according to Fig. 3, and the contour of the twisted tail has been formed by straight lines between the untwisted trailing-edge of the wing and the twisted trailing-edge of the tail. Thus the local twisting angle of the tail increases from zero at the wing trailing-edge to δ at the trailing-edge of the tail and therefore the tail is no longer plane. Bending up and down of the twisted tail around the trailing-edge of the wing allowed again to adjust different deflection angles. Three $\delta = 30°$ twisted tailes with deflection angles $\varepsilon = -5°$, $0°$ and $5°$ have been manufactured from carbon-fibre composite material in order to achieve the same stiffness as the thin sheet metal tails.

The absolute dimensions of the windtunnel model were $b = 700$ mm and $c = 140$ mm. The thickness of the plane and twisted tails was 3 mm.

2.2 *Test program*

The experimental investigations have been carried out in the 1.3 m low-speed windtunnel of the Institut für Strömungsmechanik at TU Braunschweig. The free stream velocity was $V = 40$ m/s corresponding to a Reynoldsnumber, based on the wing chord, of $Re = V \cdot c/\nu = 3.7 \cdot 10^5$.

For the wing alone as well as for all wing-tail-configurations shown in Fig. 4 three-component measurements have been carried out for deflection angles $\varepsilon = -5°$, $0°$ and $+5°$ in the angle of attack range

$$-3° \leq \alpha \leq +20°.$$

For the wing-tail-configuration F with the $\delta = 30°$ twisted tail and deflection angles $\varepsilon = -5°$, $0°$ and $+5°$ six-component measurements have been carried out in the angle of attack range

$$-5° \leq \alpha \leq +10°$$

and for angles of sideslip

$$-8° \leq \beta \leq +20°.$$

The windtunnel data have been reduced by applying the experimental coordinate system shown in Fig. 5. The aerodynamic coefficients have been based on the actual area S and the mean aerodynamic chord $\bar{c}$ of the wing-tail-configuration under consideration. As the reference point for all moments the geometric neutral point N_{25W} of the wing alone was chosen for all wing-tail-configurations. All stability considerations in this paper are based on the assumption that the centre of gravity is located at the geometric neutral point N_{25W} of the wing alone. If this is not the case the described stability differences between the wing alone and the wing-tail-configurations are still valid, but the amount of stability is different.

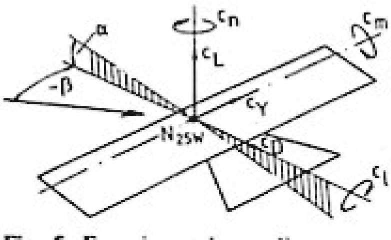

Fig. 5. Experimental coordinate system for windtunnel data reduction

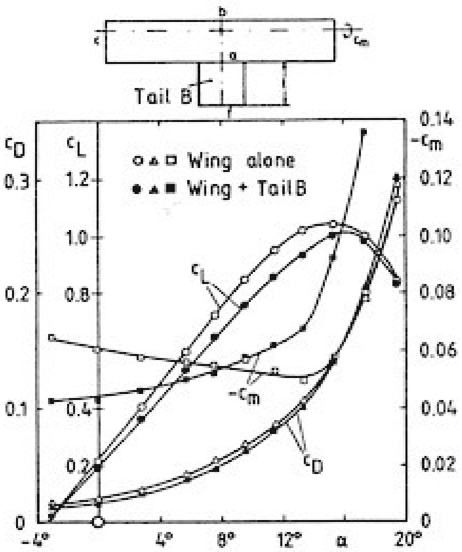

Fig. 6. Aerodynamic characteristics of the rectangular wing $A = b/c = 5$ alone and the wing-tail B-configuration ($a/c = 0.5$; $f/a = 1.0$; $l/c = 1.0$) in symmetrical flow

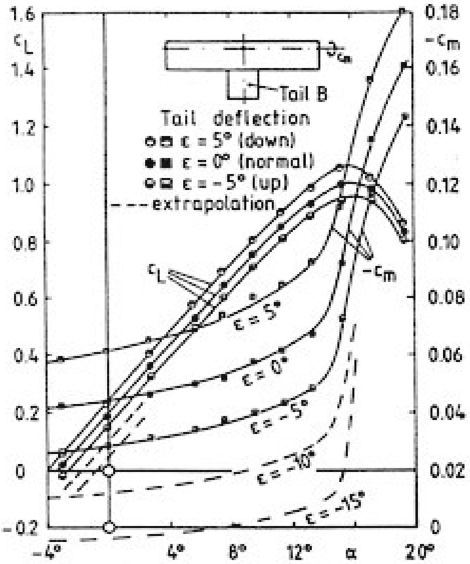

Fig. 7. Effect of tail deflection ε on the lift and pitching moment characteristics. Rectangular wing $A = 5$, tail B($a/c = 0.5$; $f/a = 1.0$; $l/c = 1.0$; ε variable), symmetrical flow

3 Results

3.1 Longitudinal motion

3.1.1 Basic function of the tail

Typical results of three-component measurements on the rectangular wing $A = 5$ without and with tail are shown in Fig. 6. Tail B has been chosen, since it has a very simple quadratic geometry with $l = 2\,a = 2\,f = c$ and $S = 1.2\,S_W$, which may be regarded as the basic tail of the investigated series, according to Fig. 4 and Table 1. For the wing alone the usual linear slopes of lift and pitching moment coefficient as well as the nonlinear dependency of the drag coefficient on the angle of attack turn out. The pitching moment slopes are $dc_m/d\alpha > 0$ and correspondingly $dc_m/dc_L > 0$ and this indicates the longitudinal instability of the wing alone.

Adding tail B to the wing leads to an increase of lift (and drag) at constant angle of attack. Nevertheless the corresponding aerodynamic coefficients are reduced. Since the aerodynamic coefficients are based on the total area of the wing-tail-configuration the increase of area leads to a more important contribution than the increase of lift (and drag). This means that the production of additional lift by the tail is less effective than the lift generation by the wing alone. The tail works in the downwash field of the wing and therefore its effectiveness with respect to the lift production is reduced. Concerning the pitching moment the slope dc_m/dc_L is negative for the wing-tail B-configuration. This means that the configuration is now stable. By adding the tail to the wing longitudinal stability is considerably improved.

Concerning the control effectiveness of the wing-tail B-configurations, Fig. 7 shows some results of three-component measurements for three different tail deflections $\varepsilon = -5°$ (up), 0° (normal) and 5° (down). By the deflections of the tail up and down the lift and pitching moment curves $c_L(\alpha)$ and $c_m(\alpha)$ are shifted parallel. This means that the zero-lift angle of attack α_0 as well as the pitching moment at zero lift $c_{m0} = c_m(c_L = 0)$ can be varied by means of such deflections ε. Therefore the tail of a bird acts as an elevator to control the longitudinal motion. For a given position of the centre of gravity, which is assumed here to be located in the geometric neutral point N_{25W} of the wing alone, an equilibrium state

$$c_m = c_{m0}(\varepsilon) + \frac{dc_m}{dc_L} \cdot c_L = 0 \tag{1}$$

can be achieved by a proper adjustment of the deflection angle ε. Fig. 7 shows some extrapolation of the pitching moment curves outside the measured range of deflection angles. Positive values of c_{m0} which are necessary for positive lift coefficients at equilibrium are achieved for negative deflection angles. The longitudinal stability is kept for different tail deflections.

The present results indicate that for symmetrical flow conditions the tail of a bird acts as a horizontal stabilizer and as an elevator in the same way as in conventional airplanes.

3.1.2 Effect of tail length

The aerodynamic characteristics of the wing-tail-configuration under consideration are shown in Fig. 8 for different tail lengths in comparison with those for the wing alone. With increasing length of the tail, corresponding to a simultaneous increase of the tail area, the lift coefficient c_L is reduced for constant angle of attack α. The lift curve slope $dc_L/d\alpha$ is also reduced and this is the well known effect of the aspect ratio which decreases with increasing area of the tail.

Concerning stability the negative pitching moment slope increases with the length of the tail. The corresponding position of the aerodynamic centre $x_{ac} - c/4 = -dc_m/dc_L$ is plotted in Fig. 9a as a function of the tail length. For a small tail of length $l/c \approx 0.2$ already the configuration becomes stable and the stability increases linearly with the length of the tail. Due to the tail the aerodynamic centre is shifted rearwards. The effectiveness of these tails with respect to control is shown in Fig. 9b. It turns out that both the control effectiveness with respect to lift and the control effectiveness with respect to pitching moment are independent of the tail length.

AVAILABLE PLANS & REFERENCE MATERIAL

Tailless Aircraft Bibliography

My book containing several thousand annotated entries and appendices listing well over three hundred tailless designers/creators and their aircraft is no longer in print. I expect *eventually* to make available on disc a fairly comprehensive annotated and perhaps illustrated listing of pre-21st century tailless and related-interest aircraft documents in PDF format. Meanwhile, I will continue to provide information from my files to serious researchers. I'm sorry for the continuing delay, but life happens.

Serge Krauss, Jr. skrauss@ameritech.net
3114 Edgehill Road
Cleveland Hts., OH 44118 (216) 321-5743

Books by Bruce Carmichael:

Personal Aircraft Drag Reduction: $30 pp + $17 postage outside USA: Low drag R&D history, laminar aircraft design, 300 mph on 100 hp.

Ultralight & Light Self Launching Sailplanes: $20 pp: 23 ultralights, 16 lights, 18 sustainer engines, 56 self launch engines, history, safety, prop drag reduction, performance.

Collected Sailplane Articles & Soaring Mishaps: $30 pp: 72 articles incl. 6 misadventures, future predictions, ULSP, dynamic soaring, 20 years SHA workshop.

Collected Aircraft Performance Improvements: $30 pp: 14 articles, 7 lectures, Oshkosh Appraisal, AR-5 and VMAX Probe Drag Analysis, fuselage drag & propeller location studies.

Bruce Carmichael brucehcarmichael@aol.com
34795 Camino Capistrano
Capistrano Beach, CA 92624 (949) 496-5191

VIDEOS AND AUDIO TAPES

(ed. – These videos are also now available on DVD, at the buyer's choice.)

VHS tape containing First Flights "Flying Wings," Discovery Channel's The Wing Will Fly, and ME-163, SWIFT flight footage, Paragliding, and other miscellaneous items (approximately 3½+ hours of material).

Cost:	$8.00 postage paid
Add:	$2.00 for foreign postage

VHS tape of Al Bowers' September 19, 1998 presentation on "The Horten H X Series: Ultra Light Flying Wing Sailplanes." The package includes Al's 20 pages of slides so you won't have to squint at the TV screen trying to read what he is explaining. This was an excellent presentation covering Horten history and an analysis of bell and elliptical lift distributions.

Cost:	$10.00 postage paid
Add:	$ 2.00 for foreign postage

VHS tape of July 15, 2000 presentation by Stefanie Brochocki on the design history of the BKB-1 (<u>B</u>rochocki,<u>K</u>asper,<u>B</u>odek) as related by her father Stefan. The second part of this program was conducted by Henry Jex on the design and flights of the radio controlled Quetzalcoatlus northropi (pterodactyl) used in the Smithsonian IMAX film. This was an Aerovironment project led by Dr. Paul MacCready.

Cost:	$8.00 postage paid
Add:	$2.00 for foreign postage

An Overview of Composite Design Properties, by Alex Kozloff, as presented at the TWITT Meeting 3/19/94. Includes pamphlet of charts and graphs on composite characteristics, and audio cassette tape of Alex's presentation explaining the material.

Cost:	$5.00 postage paid
Add:	$1.50 for foreign postage

VHS of Paul MacCready's presentation on March 21,1998, covering his experiences with flying wings and how flying wings occur in nature. Tape includes Aerovironment's "Doing More With Much Less", and the presentations by Rudy Opitz, Dez George-Falvy and Jim Marske at the 1997 Flying Wing Symposiums at Harris Hill, plus some other miscellaneous "stuff".

Cost:	$8.00 postage paid in US
Add:	$2.00 for foreign postage

VHS of Robert Hoey's presentation on November 20, 1999, covering his group's experimentation with radio controlled bird models being used to explore the control and performance parameters of birds. Tape comes with a complete set of the overhead slides used in the presentation.

Cost :	$10.00 postage paid in US
	$15.00 foreign orders

FLYING WING SALES

BLUEPRINTS – Available for the Mitchell Wing Model U-2 Superwing Experimental motor glider and the B-10 Ultralight motor glider. These two aircraft were designed by Don Mitchell and are considered by many to be the finest flying wing airplanes available. The complete drawings, which include instructions, constructions photos and a flight manual cost $250 US delivery, $280 foreign delivery, postage paid.

U.S. Pacific (559) 834-9107
8104 S. Cherry Avenue mitchellwing@earthlink.net
San Bruno, CA 93725 http://home.earthlink.net/~mitchellwing/

COMPANION AVIATION PUBLICATIONS

EXPERIMENTAL SOARING ASSOCIATION

The purpose of ESA is to foster progress in sailplane design and construction,which will produce the highest return in performance and safety for a given investment by the builder. They encourage innovation and builder cooperation as a means of achieving their goal. Membership Dues: (payable in U.S. currency)

United States	$20 /yr	Canada	$25 /yr
All other Countries	$35 /yr	Pacific Rim	$35 /yr
Electronic Delivery	**$10 /yr**	U.S. Students	Free

(Students FREE if full-time student as defined by SSA.)

Make checks payable to: Sailplane Homebuilders Association, & mail to Murry Rozansky, Treasurer, 23165 Smith Road, Chatsworth, CA 91311.